# MHD Stability of Advanced Tokamak Scenarios with Reversed Central Current: An Explanation of the "Current Hole"

G. T. A. Huysmans,[1] T. C. Hender,[2] N. C. Hawkes,[2] and X. Litaudon[1]
[1]*Association Euratom-CEA, Cadarache, F13108, France*
[2]*Euratom/UKAEA Fusion Association, Culham Science Centre, Abingdon, Oxon OX14 3DB, United Kingdom*
(Received 27 July 2001; published 27 November 2001)

A region of zero current density in the plasma center has been observed in the advanced tokamak scenarios with off-axis lower-hybrid current drive in the JET and JT-60U tokamak experiments. Significantly, the central current density does not become negative, although this is expected based on conventional current diffusion. In this paper, it is shown that the zero central current density and the absence of negative central current can be explained by the influence of a resistive kink magnetohydrodynamic instability.

DOI: 10.1103/PhysRevLett.87.245002 PACS numbers: 52.55.Fa, 52.30.Cv, 52.65.Kj

In the advanced tokamak scenarios, the plasma is characterized by an internal transport barrier (ITB), a region of improved confinement of heat and particles [1–3]. Plasmas with a very low or negative slope of the safety factor ($q$) in the plasma center have been found to have a particularly low heating power threshold for inducing the ITB [4–7]. Such reversed $q$ profiles imply a current profile with an off-axis maximum. To obtain the required current profiles, the diffusion of the current density towards the plasma center is reduced by heating the plasma while the current is ramping up. The central current density can be further reduced by applying a noninductively driven current off-axis.

Recently, in the advanced tokamak scenarios in JET with off-axis Lower-Hybrid current drive (LHCD) during the current ramp, a relatively large central region (with a radius of ~20 cm) with a zero or very small toroidal current has been observed [8]. A similar phenomenon has been observed in the advanced scenarios in the JT-60U tokamak [9,10] where it has been named the "current hole." A detailed study of the motional Stark effect measurements (MSE) of the poloidal magnetic field in JET has shown [8] that with the application of the off-axis Lower hybrid-current drive (LHCD), the central current density reduces to zero but, significantly, does not become negative (within error bars). Simulations of the current diffusion during this phase show that the central current is expected to become (transiently) negative in the plasma center [11]. Experimentally, however, the central current density appears to be "clamped" at zero. In this Letter, the magnetohydrodynamic (MHD) stability, both linear and nonlinear, of current profiles with a negative central current density is analyzed. In the nonlinear simulation, a full current ramp phase is modeled including the influence of MHD instabilities on the evolution of the current profile. It is shown that the "clamping" of the central current density can be explained by the influence of an $n = 0$ resistive kink instability.

For the analysis of the MHD stability of the current profiles with negative central current density the well-known reduced MHD model [12] is used. The reduced MHD equations describe the time evolution of the electrostatic potential $\phi$, the poloidal flux $\psi$, and the pressure $p$ in a quasicylindrical geometry:

$$\frac{\partial p}{\partial t} = -\nabla\varphi \cdot \nabla\phi \times \nabla p + \kappa_\perp \nabla_\perp^2 p + \kappa_\| \nabla_\|^2 p + S, \qquad \frac{\partial \psi}{\partial t} = F\nabla\varphi \cdot \nabla\phi + \nabla\varphi \cdot \nabla\psi \times \nabla\phi + \eta(J_\| - J_{CD}), \tag{1}$$

$$\frac{\partial w}{\partial t} + \nabla\varphi \cdot \nabla\phi \times \nabla w = F\nabla\varphi \cdot \nabla J_\| + \nabla\varphi \cdot \nabla\psi \times \nabla J_\| - 2\nabla\varphi \times \nabla R \cdot \nabla p, \qquad J_\| = \nabla_\perp^2 \psi, \qquad w = \nabla_\perp^2 \phi,$$

where $F = R_0 B_0$, $R_0$ is the major radius, $B_0$ the toroidal field, $J_\|$ the parallel current density, $J_{CD}$ is the non-Ohmic driven current density, $\eta$ the resistivity, $\kappa_{\perp,\|}$ the perpendicular and parallel heat conductivity, $S$ a heat source, and the $\varphi$ toroidal angle. All quantities are normalized to the toroidal magnetic field, the minor radius $a$, and the Alfvén time $\tau_A = a\sqrt{\mu_0 \rho_0}/B_0$ ($\rho_0$ is the mass density on axis). The standard linear resistive MHD codes in toroidal geometry such as CASTOR [13] cannot be used for this problem because they use a flux coordinate system which is not well defined with a negative central current density. The reduced MHD codes used here [14] are based on a conventional polar coordinate system.

For the linear MHD analysis, a set of analytic current density profiles is considered with a variable central current density: $j(r) = j_a(1 - r^4) - j_b(1 - r^2)^8$ (where $r$ is the normalized minor radius). The pressure is taken to be small such that it does not contribute to the growth rate. The equilibria are found to be unstable to a resistive MHD mode when the central current density becomes negative. The toroidal, $n$, and poloidal mode number, $m$, of the instability are $n = 0$ and $m = 1$, respectively. The $n = 0/m = 2$ mode is also unstable but with a smaller growth rate. Figure 1a shows the growth rates of the two instabilities as a function of the normalized current density on axis $\tilde{j}(0) = (j_a - j_b)/j_a$. The scaling of the growth rate as a function of the resistivity is shown in Fig. 1b. The growth rate scales like $\lambda \sim \eta^{1/3}$ which identifies the mode as a resistive kink mode. The radial structure of the $n/m = 0/1$ instability is shown in Fig. 2. The mode is localized inside the radius where the poloidal field goes to zero, i.e., where the safety factor $q$ goes to infinity (the $q = \infty$ surface is the rational surface for the $n = 0$ modes). The electric potential $\phi$ of the $m = 1$ mode in Fig. 2 implies a toroidally symmetric vortex flow across the plasma axis ($\vec{v} = B_0 \times \nabla\phi/B_0^2$).

To evaluate the effect of the resistive kink mode on the evolution of the current profile, a full current ramp phase has been modeled using the nonlinear reduced MHD equations (1). For typical JET plasma parameters, a two second current ramp is of the order of $10^7$ Alfvén times. The required numerical time step is $\leq 1\tau_A$ in the (quasi) linear phase (a fraction of that in the full nonlinear calculation). To reduce the computation time, the Alfvén time is increased such that the current ramp phase is about $10^6\tau_A$; the current ramp rate and the magnetic Reynolds number are adjusted accordingly. The current ramp is controlled through a feedback scheme (as in the experiment) on the time derivative of the poloidal flux at the boundary. In this way the time evolution of the total current can be prescribed; here a constant current ramp rate is prescribed. The driven current $J_{CD}(r, t)$ (i.e., the LHCD) is modeled by assuming a fixed radial shape and amplitude of the driven current localized between $0.2 < r < 0.7$. The current ramp is started with a parabolic current profile with a total current such that $q$ at the boundary is 100. The driven current is applied at $t = 4 \times 10^5$ Alfvén times, the minimum in the $q$ profile at this time is about $q_{\min} = 7$. The pressure is assumed to be small, such that it has no influence on the MHD instability [$p(r) = 10^{-6}(1 - r^2)$]. (The pressure profile is included to evaluate the effect of the MHD instability on the profile shape.) The profile of the resistivity scales like $p^{-3/2}$ at $t = 0$. The heating due to the LHCD and the subsequent reduction in resistivity is not taken into account. (The present modeling aims to qualitatively reproduce the key features observed in the experiment and is not meant to be an exact quantitative model.)

First, the evolution of the current profile is calculated using only the $n = 0$ and $m = 0$ harmonics. This excludes the effect of the resistive kink mode and models a conventional current ramp. Figure 3a shows the evolution of the toroidal current density on the axis as a function of time during the full current ramp for 3 values of the amplitude of the driven current. In the initial Ohmic part of the current ramp ($0 < t < 4 \times 10^5\tau_A$) the current diffuses inwards raising the central current density. The driven current causes a reversal of the sign of the electric field in the central part of the plasma, which reduces the central current density. If the amplitude of the driven current is large enough, relative to the Ohmic current, the central part of the current density can become negative. This shows that with conventional current diffusion in combination with an off-axis driven current, the central current density can become (transiently) negative. Because of the continued current ramp in this scenario, the Ohmic current increases with time, which eventually forces the central current density back to a positive value. For the profile shapes used here, the minimum driven current required to obtain a negative central current density is about the value of the total Ohmic current (the exact value depending on the chosen resistivity). Note that the central current density can become negative even if the driven current extends up to the axis.

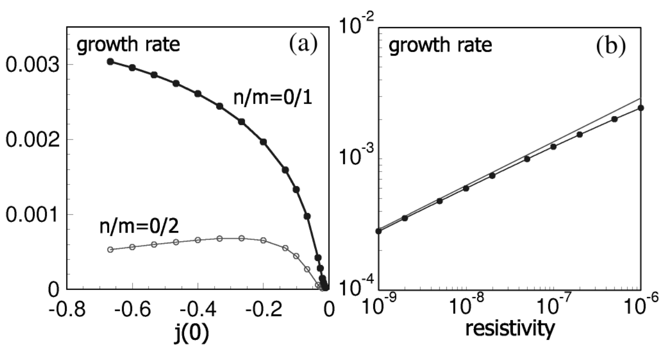


FIG. 1. (a) The growth rates of the $n/m = 0/1$ and $n/m = 0/2$ resistive kink modes as a function of the normalized central current density [$\tilde{j}(r = 0)$] for a resistivity $\eta = 10^{-6}$. The modes are stable for positive central current density. (b) The scaling of the $n/m = 0/1$ growth rate with resistivity for $\tilde{j}(r = 0) = -0.33$ shows an $\eta^{1/3}$ scaling indicative of a resistive kink mode. The thin line indicates the $\eta^{1/3}$ scaling.

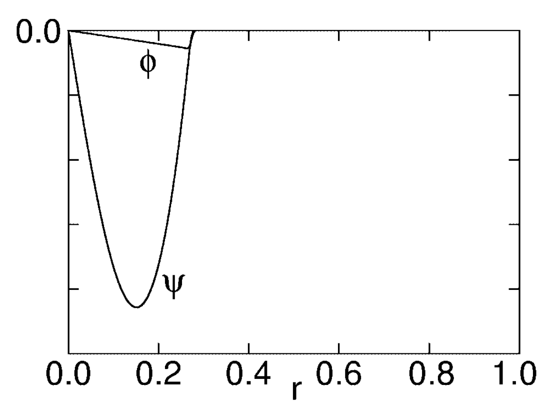


FIG. 2. The radial mode structure of the $n/m = 0/1$ resistive kink mode.

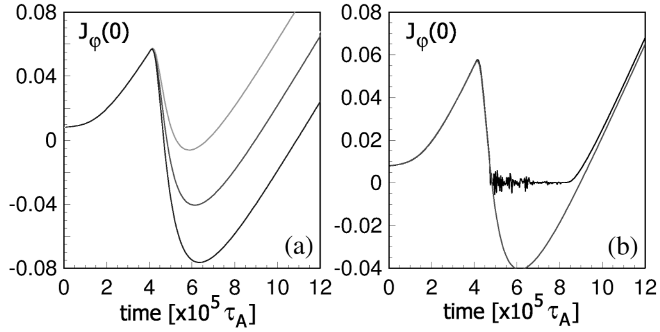


FIG. 3. (a) The evolution of the central current density during the current ramp with an off-axis source of LHCD current drive, for 3 values of the driven current [$I_{CD} = 1.2$, 1.6, and $2 \times I_p(t = 4 \times 10^5 \tau_A)$]. The resistivity on axis is $\eta(0) = 2 \times 10^{-7}$, the viscosity $\nu = 2 \times 10^{-8}$, the perpendicular heat conductivity $\kappa_\perp = 10^{-6}$. (b) Comparison of the evolution of the current density on axis with and without the influence of the $n/m = 0/1$ resistive kink mode.

Next, the effect of the $n/m = 0/1$ resistive kink mode on the evolution of the current profile is evaluated self-consistently, by including the $n/m = 0/0$ and $n/m = 0/1$ harmonics in the calculation. The results shown are from quasilinear calculations using two harmonics. Including more poloidal harmonics does not significantly change the nonlinear behavior. In this scenario, the current density first becomes negative off axis at $r = 0.23$ at $t = 4.27 \times 10^5 \tau_A$ while the current density on axis is still positive. The resistive kink mode starts to grow as soon as the off-axis negative current compensates the positive current on axis ($t = 4.45 \times 10^5 \tau_A$), such that there is a radius where the poloidal field $B_p$ vanishes, i.e., a $q = \infty$ surface appears [$B_p = \int j(r')r'\,dr'/2\mu_0 r$]. Figure 4 shows the energy of the $n/m = 0/1$ mode as a function of time. In the initial phase, the mode grows exponentially with a growth rate of $2.6 \times 10^{-3} \tau_A^{-1}$. It takes about $3 \times 10^4$ Alfvén times to reach a large enough amplitude for the mode to have an effect on the current profile. (However, this time does depend on the level to which the $n/m = 0/1$ perturbation has decayed in the stable phase of the current ramp.) After this linear phase, the amplitude of the resistive kink mode saturates. With the continued ramp of the current, the relative amplitude of the driven current is reduced. Consequently, the average amplitude of the mode (which is continuously present) decreases slowly. When the driven current is too small to drive a negative current in the center, the $q = \infty$ surface disappears and the mode decays exponentially.

The evolution of the central current density with and without the effect of the resistive kink mode is shown in Fig. 3b. Clearly, the MHD instability has a large influence on the evolution of the central current density profile. It removes the current density within a radius $r < 0.3$–$0.35$. As a consequence, the mode "clamps" the current density on axis to zero. Thus, the current profiles with a zero central current density and the absence of a negative current density as observed in the JET [8] and JT60-U experiments [8,9] can be explained by the action of a nonlinearly saturated resistive kink mode.

The evolution of the current profile at the start of the saturation phase is shown in more detail in Fig. 5. At the end of the linear phase, the plasma center starts moving outwards (corresponding to the flow pattern of the linear instability) up to the $q = \infty$ surface where a large current spike forms (at $t = 4.74 \times 10^5 \tau_A$). This current spike decays in about $5000 \tau_A$. After this a nonlinear oscillation can be seen with periodically returning current spikes. This oscillation can also be clearly seen on the time traces of the energy of the instability (Fig. 4) and the central current density (Fig. 3b). The oscillation has a reasonably well-defined frequency $1/f \sim 8 \times 10^3 \tau_A$. This frequency decreases with decreasing resistivity approximately as $f \sim \eta^{0.6}$. The maximum amplitude of the oscillation at $r \sim 0.25$ in the current profile is $\sim$5% of the maximum current density (at $r = 0.45$). The amplitude increases approximately linearly with the amplitude of the off-axis current drive. The phase of the oscillation is constant across the radius. The oscillation is due to the competing effects

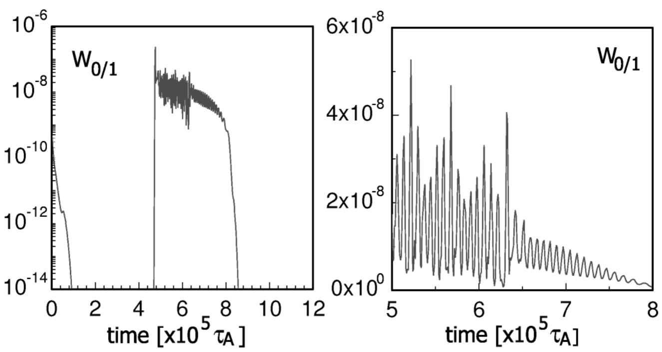


FIG. 4. The evolution of the energy of the $n = 0/m = 1$ resistive kink mode during the current ramp phase.

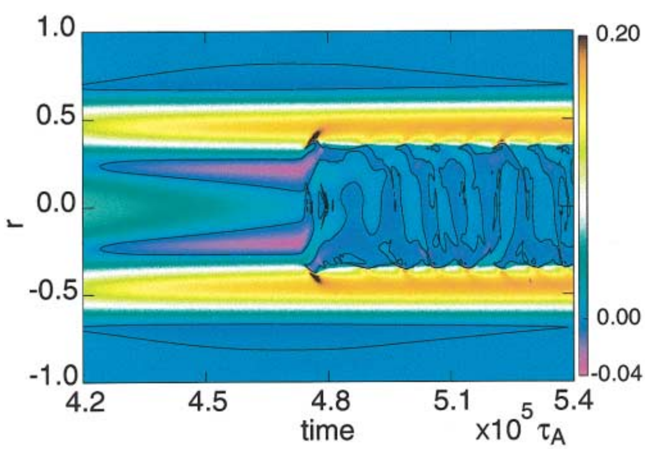


FIG. 5 (color). A contour plot of the evolution of the current density as a function of radius and time. The black contour indicates zero current density.

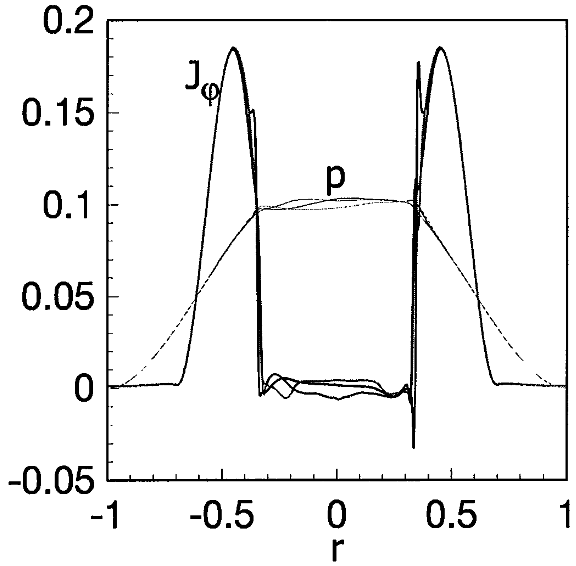


FIG. 6. The profiles of the toroidal current density and the pressure $[p(r)/8 \times 10^{-6}]$ as a function of radius at $t = 5.76$, 5.78, and $5.80 \times 10^5 \tau_A$.

of the MHD instability and the off-axis driven current. The resistive kink mode tends to bring the current density back to zero and remove the $q = \infty$ surface after which the mode amplitude decays. The off-axis driven current reduces the central current density and reintroduces the $q = \infty$ rational surface. The shape of the current profile and the pressure profile in the presence of the resistive kink mode are shown in Fig. 6. The current profile is flat inside the radius $r < 0.30-0.35$ and has an extremely large current gradient just outside this region. The MHD instability also removes the pressure gradient in the central part. Apart from the initial fast removal of the central pressure gradient, the instability does not lead to repeated sawtoothlike collapses, but it keeps the central pressure profile flat.

In conclusion, the current profiles with zero central current, and the absence of negative central current, observed in some of the advanced tokamak scenarios in both JET and JT-60U can be explained by the influence of a resistive kink MHD instability on the evolution of the current profiles. The off-axis driven current through Lower-Hybrid current drive tends to create a (transiently) negative current density in the plasma center. An $n/m = 0/1$ resistive kink mode becomes unstable when the negative current creates a zero in the poloidal field (i.e., $q = \infty$). This instability removes the negative current in the center and flattens the central current profile to zero. The mode is continuously present as long as the off-axis current drive is sufficiently strong, compared to the Ohmically driven current, to create a negative current density in the plasma core.

Because of the toroidal symmetry of the instability, the toroidal rotation does not contribute to the frequency of the mode. This will make the direct experimental observation of the instability more difficult. The numerical simulations do predict some features of the $n = 0$ resistive kink mode that might be observed. Apart from the flattening to zero of the core current profile on a fast time scale, the simulated current profiles also show a very large gradient in the current profile just outside the region with zero current. The sharp transition observed in the JET MSE data [8] at the edge of the current hole does indicate the presence of a large current gradient. In addition, the numerical simulations show a nonlinear oscillation of the central current density with a period of the order of $\sim 5 \times 10^4$ Alfvén times which translates to several ms for typical JET plasma parameters. The phase of this oscillation is constant across the radius, the amplitude increases linearly with the off-axis current drive. Detailed measurements of the current profile on a fast time scale with the MSE diagnostic may indicate the presence of the instability.

The simulations presented, using the reduced MHD equations in cylindrical geometry, qualitatively explain the observations of the zero current density in the JET and JT-60U experiments. A more quantitative comparison with experimental observations will require simulations in the full toroidal geometry.

This work was performed under the European Fusion Development agreement and was partly supported by EURATOM and the U.K. Department of Trade and Industry.

[1] F. M. Levington *et al.,* Phys. Rev. Lett. **75**, 4417 (1995).
[2] E. J. Strait *et al.,* Phys. Rev. Lett. **75**, 4421 (1995).
[3] C. Gormezano and the JET Team, in *Fusion Energy 1996: Proceedings of the 16th International Conference, Montreal, 1996* (IAEA, Vienna, 1997), Vol. 1, p. 487.
[4] Y. Kamada, Plasma Phys. Controlled Fusion **42**, A65 (2000).
[5] E. J. Synakowski, Plasma Phys. Controlled Fusion **39**, B47 (1997).
[6] K. H. Burrell, Phys. Plasmas **4**, 1499 (1997).
[7] C. D. Challis *et al.,* in Proceedings of the 28th EPS Conference on Plasma Physics and Controlled Fusion, Madeira, Portugal, 2001 (to be published).
[8] N. C. Hawkes *et al.,* Phys. Rev. Lett. **87**, 115001 (2001).
[9] T. Fujita *et al.,* Phys. Rev. Lett. (to be published).
[10] M. Kikuchi, in Ref. [7].
[11] T. J. J. Tala *et al.,* in Ref. [7].
[12] S. E. Kruger, C. C. Hegna, and J. D. Callen, Phys. Plasmas **5**, 4169 (1998).
[13] W. Kerner, J. P. Goedbloed, G. T. A. Huysmans, S. Poedts, and E. Schwartz, J. Comput. Phys. **142**, 271 (1998).
[14] D. N. Borba, K. S. Riedel, W. Kerner, G. T. A. Huysmans, M. Ottaviani, and P. J. Schmid, Phys. Plasmas **1**, 3151 (1994).